Journal of Coastal Research	SI	59	150-155	West Palm Beach, Florida	2011

Analysis of Packery Channel Public Access Boat Ramp Shoreline Failure

Christopher W. Reed[†] and Lihwa Lin[‡]

[†]URS Corporation
1625 Summit Lake Drive
Tallahassee, FL 32317, USA
Chris_reed@urscorp.com

[‡]U.S. Army Engineer Research & Development Center
3909 Halls Ferry Road
Vicksburg, MS 39180-6199, USA

www.cerf-jcr.org

ABSTRACT

REED, C.W. and LIN, L., 2011. Analysis of Packery Channel Public Access Boat Ramp Shoreline Failure. *In:* Roberts, T.M., Rosati, J.D., and Wang, P. (eds.), *Proceedings, Symposium to Honor Dr. Nicholas C. Kraus,* Journal of Coastal Research, Special Issue, No. 59, pp. 150-155. West Palm Beach (Florida), ISSN 0749-0208.

The shoreline stabilization adjacent to the public access boat ramp in the Packery Channel basin has been damaged in two separate events. For the shoreline damage at the boat ramp bulkhead, toe scour is the likely mechanism for failure. Typical sources of hydrodynamic forcing that can lead to toe erosion include storm currents, locally generated storm waves, and offshore storm waves propagating into the basin through Packery Channel. Quantitative analysis of storm induced wind generated waves and currents eliminated them as possible causes of the damage. However, photographic and movie evidence indicate the presence of low-frequency low-amplitude waves propagated into the basin and impacted the boat ramp. The Coastal System Model (CMS) was used to simulate a range of these low-frequency low-amplitude waves and the results demonstrated that these waves could produce sufficient flows in the vicinity of the boat ramp shoreline to cause the damage. Subsequent modeling was used to develop design criteria for additional shoreline stabilization.

ADDITIONAL INDEX WORDS: *Coastal hydrodynamics, flow modeling, wave modeling, Packery Channel.*

INTRODUCTION

The shoreline stabilization adjacent to the public access boat ramp in the Packery Channel basin has been damaged in two separate events. In August, 2006 the articulated mats on the east side of the eastern bulkhead failed and slumped into the channel. A view of the damaged articulated mats are shown in Figure 1a. The damage was likely associated with tropical storm Erin. The damage to the articulated mats was sufficiently severe and the repositioning of the mats was not feasible. Therefore, an interim shoreline re-stabilization measure consisting of filling in the damaged area with cobble size rock was implemented. This approach was intended to temporarily protect the damaged area until a complete analysis and design could be developed. The construction of the complete solution was to be implemented simultaneously with the construction of the parking area and related infrastructure adjacent to the boat ramp. However, on a second incident, in September, 2007, prior to completion of the design and construction of the final remedy the rock fill failed and slumped into the channel. A view of the damaged fill is shown in Figure 1b. The damage was likely associated with hurricane Ike. An investigation of the potential causes of the damage was undertaken after the second failure.

DOI: 10.2112/SI59-015.1 received 1 October 2009; accepted 15 June 2010.
© Coastal Education & Research Foundation 2011

WAVE AND CURRENT CONDITIONS LEADING TO FAILURES

The initial damage to the shoreline protection is typically due to scour near the toe of the protective mats. Often, sediment at the toe of the shoreline protection is eroded and the structure subsequently slips into the scour hole. For the shoreline damage at the boat ramp bulkhead, toe scour is the likely mechanism for failure. In the vicinity of the boat ramp bulkhead, typical sources of hydrodynamic forcing that can lead to toe erosion include storm currents, locally generated storm waves, and offshore storm waves propagating into the basin through Packery Channel.

However, assuming that toe scour was the cause of the failure, the hydrodynamic forces leading to the toe scour are not likely high current speeds or wind-generated waves. The geometry of the bulkhead and shoreline preclude large currents speeds from developing in the vicinity of the failure. The bulkhead causes the channel flow to divert away from the shoreline, creating a 'quiet' zone in the corner formed by the shoreline and bulkhead. Furthermore, it is unlikely that sufficiently large wind-generated waves could be developed in the area to cause the scour. The basin within which the boat ramp resides has a relatively small fetch, which will limit wind-generated wave growth. Also, any propagation of the wind-generated waves and swell from offshore of the channel leading to the basin will be dissipated before reaching the basin. Thus neither high currents nor wind-generated waves are likely to have been the primary cause of the

Figure 1. a) Damage to original articulated mat during tropical storm Erin. b) Damage to interim rock fill during Hurricane Ike.

Figure 2. a) Wave propagating into the bulkhead and shoreline. b) Wave surge receding from the bulkhead and shoreline.

damage, although they may have been a secondary source of hydrodynamic energy leading to the failure.

Photographic evidence of the presence of low-frequency low-amplitude waves as well as movies providing quantification of the periods associated with the waves supports the hypothesis that these waves are the primary source of damage at the boat ramp bulkhead. Figures 2a and 2b show the water surface height in the vicinity of the bulkhead as the wave propagates through the basin. The wave propagates into and away from the corner formed by the bulkhead and shoreline with a period on the order of 45 seconds. There is no wave breaking apparent, but the long-period wave acts as small surge during each passing. It appears the corner area is subject to heightened surge level from the wave, likely due to the deflection of the surge by the bulkhead.

The source of these low-frequency low-amplitude waves is not clearly identified, but one possibility is infragravity waves. Infragravity waves, originally referred to as surf-beat, have periods typically from 30 seconds to 5 minutes. It is likely that the low-frequency water level oscillations associated with infragravity waves occur during storm conditions propagated into the channel and the basin, eventually reaching the boat ramp.

A number of analyses have been conducted to quantitatively confirm the hypothesis that currents and wind-generated waves are not the primary source of the damage, and that storm-induced low-frequency low-amplitude waves are the main cause of the damage. The analyses consist of (1) simulation of storm induced currents, (2) calculation of locally generated waves for storm related winds, (3) simulation of offshore storm waves propagating into the basin and (4) the simulation of low-frequency low-amplitude waves from offshore sources.

For all of the analyses, the bathymetric data collected by Williams *et. al* (2005; 2007; this issue) was used to configure models and provide depth information for the analyses. A color coded contour plot of the bathymetric data is shown in Figure 3.

ANALYSIS

Simulation of Currents

The simulation of currents was done using the Coastal Modeling System 2D Flow model (CMS-Flow). CMS-Flow (Militello, 2004) is a process-based 2D depth-averaged hydrodynamic, sediment transport and morphology model developed by the USACE for application in and around inlets and channels. It is accessible via the Surfacewater Modeling System (SMS) graphical user interface. For this application only the hydrodynamic component of the model was implemented. A model grid was configured for the basin area consisting of 0.5 meter cell spacing. The smaller grid cells were used in and around the bulkhead to properly represent the geometry in that area. The basin grid is shown in Figure 4. Water surface elevation boundary conditions were applied at the eastern and western ends of the basin so that a 2 meter current was developed in the inlet area of the channel. Typical peak tidal currents in the channel are on the order of 1 m/s, and a 2 m/s value was adopted as representative of storm induced currents. A manning's n value of 0.03 was used for the basin. The

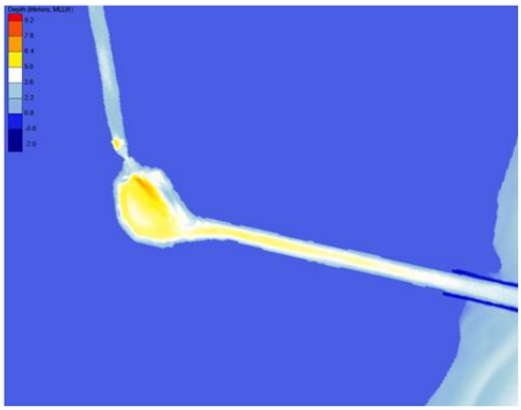

Figure 3. Bathymetric data for the channel, basin and offshore area in the vicinity of the jetties.

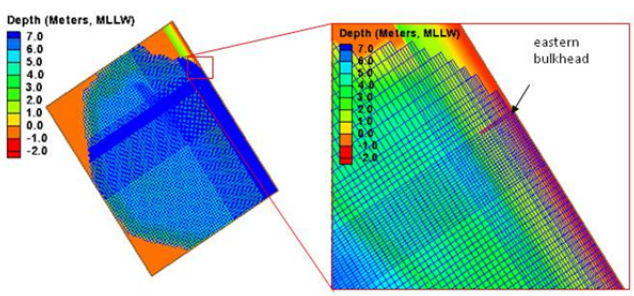

Figure 4. Views of the basin CMS Flow model grid cells.

simulated velocities in the main channel are reduced substantially by the increased cross-sectional area of the deep part of the basin. Near the boat ramp, the velocities are also reduced due to the flow diversion created by the bulkhead. The flow speeds in the corner created by the bulkhead and the shoreline are about 0.25 m/s.

Analysis of Locally Generated Wind Waves

An estimate of the locally generated wind waves was made using the wind-fetch-depth nomographs in the USACE Shore Protection Manual (USACE, 1976). These nomographs provide wave height and periods when a fetch length, water depth and wind speed are provided. The bathymetric data in Figure 3 was used to develop both a representative fetch length and water depth. The fetch used represents a distance from the boat ramp south-southwestward to the opposite shoreline, which represents the longest fetch along which waves would directly impact the damaged area. The fetch length is 230 meters. The average water depth along this fetch is approximately 2 meters. Using a representative wind speed of 80 mph, the associated wave height and period are 0.35 m and 2.8 seconds. These waves are not sufficient to cause the damage to the shoreline armoring.

Simulation of Wave Propagation from Offshore

The potential for the propagation of offshore wind generated waves and swell were evaluated using the CMS-Wave model (Lin *et al.*, 2008). CMS-Wave is a short-period wave generation and wave propagation model supported by the USACE accessible via the SMS graphical user interface. It is a steady-state, finite difference, spectral model based on the wave action balance equation and simulates depth-induced wave refraction and shoaling, current-induced refraction and shoaling, depth- and steepness-induced wave breaking, diffraction, wave growth because of wind input, and wave-wave interaction and white capping that redistribute and dissipate energy in a growing wave field. The model was configured to represent the channel starting from the tip of the jetties inland to the basin. A series of wave conditions were applied at the jetty tips and the propagation of the waves into and along the channel were simulated. An example of the resulting wave height pattern is shown in Figure 5. The waves are refracted and dissipated sufficiently such that they do not propagate the full length of the channel. A range of storm–size wave conditions were evaluated and for each case, the wave energy did not reach the basin.

SIMULATION OF LOW FREQUENCY LOW AMPLITUDE WAVES

The potential for simulation of low-frequency low-amplitude waves propagating into the basin was evaluated with hydrodynamic simulations using the CMS-Flow model. A model grid using 0.5 meter cell spacing in the vicinity of the boat ramp and 3 meter cell spacing in the surrounding areas was used to represent the channel and basin. The model grid bathymetry and extent is shown in Figure 6. The grid domain extends from the jetty tips, through the basin and includes the continuation of the channel westward beyond the basin. At the offshore boundary a time dependent water surface elevation was applied to simulate the long-period wave motion of low-frequency low-amplitude waves along the Gulf shoreline.

An amplitude of 0.20 cm and a period of 60 seconds was used

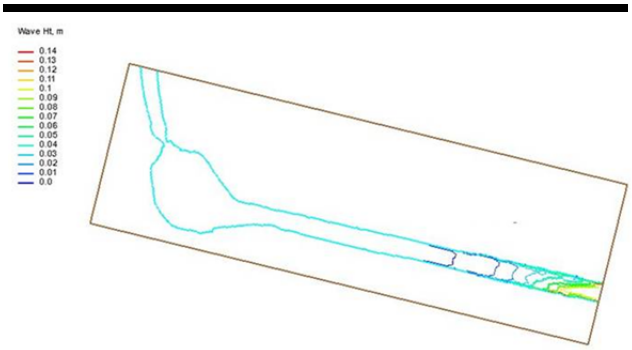

Figure 5. Offshore Wind Generated Wave Propagation into Channel.

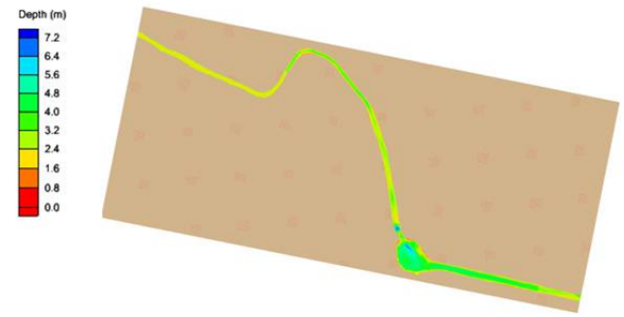

Figure 6. CMS-Flow grid for low-frequency wave analysis.

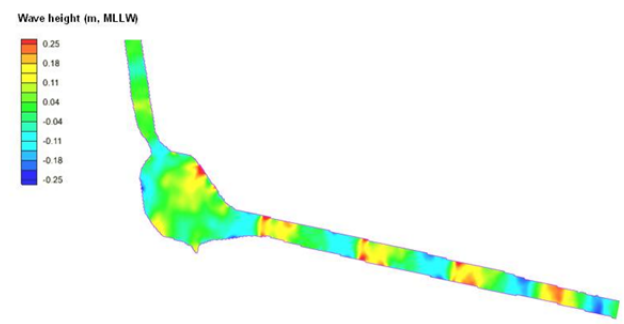

Figure 7: Simulation of low-frequency waves: instantaneous wave pattern.

for the evaluation. Figure 7 shows a color coded contour plot of the instantaneous wave heights of the propagating waves during the simulation and Figure 8 shows an instantaneous water surface profile of the waves along the channel centerline as they propagate along the channel. The yellow/red areas in the channel indicate the wave crests. It appears that the wave length is about 250 meters, and that the waves transform with steeper fronts and long shallower troughs as they propagate along the channel. The wave heights tend to decrease due to geometric spreading of the wave front as they enter the basin, but there is evidence of shoaling and/or reflection causing higher wave heights along the shoreline.

These results provide sufficient evidence that low-frequency low-amplitude offshore waves have the potential to propagate into the basin and may actual transform, reflect and shoal to yield higher wave heights than the original offshore wave amplitude.

DESIGN CONDITIONS BASED ON CMS-FLOW SIMULATIONS

Based on the conclusion in section 4.0 that low-frequency low-amplitude waves are the likely primary source of the damage, additional analysis has been completed to estimate

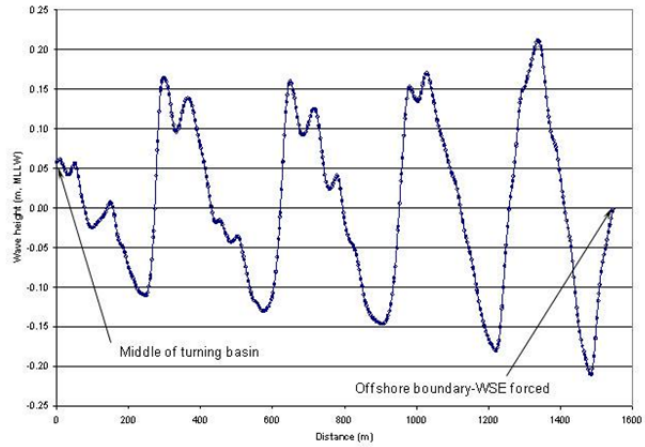

Figure 8: Wave height along the centerline of the channel

design conditions. The typical approach for developing design conditions is to review the historical record of measured wave and/or current conditions and select the design conditions based on a prescribed return interval or design life period. The modeling analysis is then used to estimate the associated velocities and associated forces. Unfortunately, very little data exists for low-frequency low-amplitude offshore waves and there is no long term record for which to base a return-period analysis. Therefore, an alternate 'worst-case' approach has been adopted. The approach consists of selecting wave conditions such that the surge in the vicinity of the bulkhead extends from MLLW to land elevation. Any larger wave induced surges would overtop the shoreline and dampen the effect of the increased surge. The distance between land elevation and MLLW in the vicinity of the boat ramp is approximately 1.6 meters, (5.25 ft).

The modeling analysis used to determine the 'worst-case' conditions consisted of applying a low-frequency low-amplitude wave at the southeastern boundary of the basin grid, simulating its propagation into the basin, and monitoring the surge at the boat ramp bulkhead and adjacent shoreline. The wave height and period were varied until a 1.6 m surge was obtained. After some experimentation and a systematic increase in the applied wave height, a 0.6 meter height with a 60 second period yielded a 1.6 meter surge at the bulkhead and shoreline. An instantaneous wave height distribution for the final simulation is shown in Figure 9. In Figure 9, the effect of the wave at the boat ramp bulkhead and shoreline is evident, as the wave surges with a peak elevation that reaches the land elevation.

In order to determine the critical surge water depth and flow speed, the simulation results were tracked at points in and around the bulkhead. The tracking points are shown in Figure 10. The time dependent speed and water depth were tracked and reviewed at each point. A typical response, as shown for Point 4 in Figure 11, indicates a peak surge occurring over about 15 seconds, during which the water surges about 1.25 meters above MLLW, with a peak velocity of 1.6 m/s.

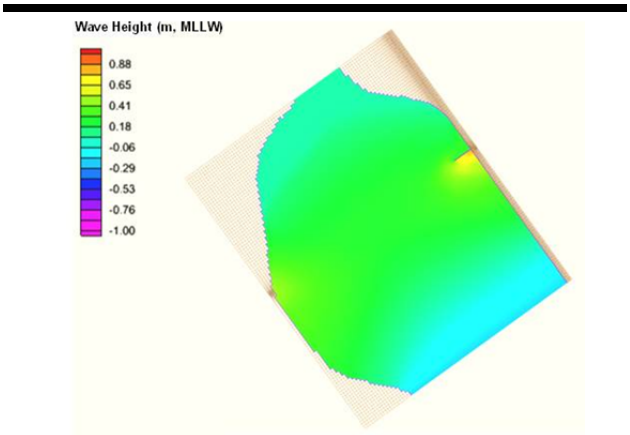

Figure 9: Wave surge as it encounters the boat ramp bulkhead.

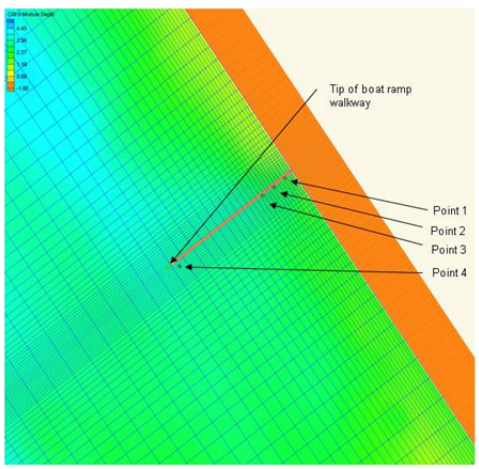

Figure 10: Location of tracking points near boat ramp bulkhead.

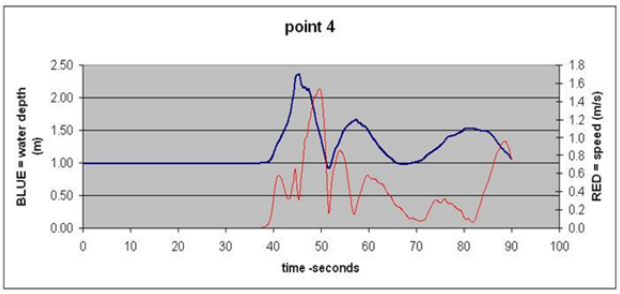

Figure 11. Surge response at Point 4.

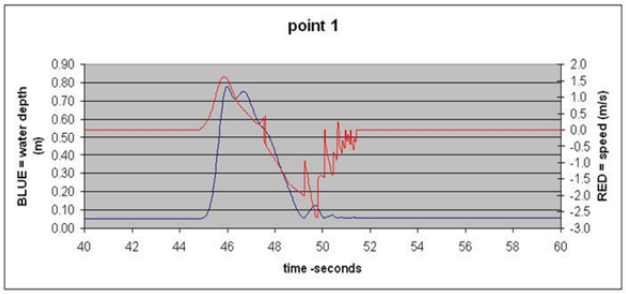

Figure 12. Surge response at Point 1.

The most critical response occurred at Point 1, which represents the highest point obtained by the surge. The response is shown in Figure 12. The maximum water depth is lower at this point in comparison with Point 4, since the bed elevation is higher at the Point 1 location. The surge peak water depth is about 0.78 meters above the bed, with the surge only lasting about 6 seconds. The peak velocity occurs as the surge is receding with a maximum value of 2.5 m/s. These values were used to determine the optimum rubble size and distribution for re-stabilizing the shoreline.

CONCLUSIONS

CMS-Flow has been successfully applied to demonstrate that low-frequency low-amplitude waves are the likely cause of the damage to the Packery Channel basin boat ramp bulkhead. The model results indicate that small amplitude long-period waves generated offshore during storms can propagate through the Packery Channel and yield sufficient energy in the vicinity of the boat ramp to cause severe damage. The wave impacts are accentuated by the geometry of the boat ramp, since the boat ramp bulkhead is perpendicular to the shoreline and the general wave direction. Design conditions could be developed, despite the lack of long term data on the occurrences of these waves, because the impact of these waves with run-up greater than the top of the boat ramp were greatly reduced.

ACKNOWLEDGMENTS

The authors are grateful to Dr. Nicholas C. Kraus for his continual support and encouragement for many years towards development and improvement of the capabilities of CMS-Flow to increase reliability of modeling for coastal inlets and navigation applications. Permission was granted by the Chief, U. S. Army Corps of Engineers to publish this information.

LITERATURE CITED

Lihwa, L.; Demirbilek, Z.; Mase, H.; Zheng, J., and Yamada, F., 2008. *CMS-Wave: A Nearshore Spectral Wave Processes Model for Coastal Inlets and Navigation Projects*, ERDC/CHL-TR-08, 132p.

Militello, A.; Reed, C. W.; Zundel, A. K., and Kraus, N. C., 2004. *Two-dimensional depth-averaged circulation model M2D: Version 2.0, Report 1: Documentation and user's guide*. ERDC/CHL TR-04-02, Vicksburg, Mississippi, US Army Engineer Research and Development Center, 128p.

United States Corps. of Engineers Staff, 1984. Shore Protection Manual, Department of the Army, USACE Publication.

Williams, D.D.; Kraus, N.C., and Anderson, C.M., 2005. Baseline and construction monitoring of Packery Channel, Corpus Christi, Texas. *Florida Shore and Beach Preservation Association*, http://www.fsbpa.com/publications.html, 16pp.

Williams, D.D.; Kraus N.C., and Anderson, C.M. 2007. Morphologic response to a new inlet, Packery Channel, Corpus Christi, Texas. *Coastal Sediments '07*, N.C. Kraus and J.D. Rosati (eds.), ASCE, 1,529-1,542.